



**HAL**  
open science

## **Bulk modulus evolution of thermoset resins during crosslinking: Is a direct and accurate measurement possible?**

Mael Péron, Vincent Sobotka, Nicolas Boyard, Steven Le Corre

### ► **To cite this version:**

Mael Péron, Vincent Sobotka, Nicolas Boyard, Steven Le Corre. Bulk modulus evolution of thermoset resins during crosslinking: Is a direct and accurate measurement possible?. *Journal of Composite Materials*, 2016, 51 (4), pp.463-477. 10.1177/0021998316647119 . hal-02387387

**HAL Id: hal-02387387**

**<https://hal.science/hal-02387387>**

Submitted on 2 Dec 2019

**HAL** is a multi-disciplinary open access archive for the deposit and dissemination of scientific research documents, whether they are published or not. The documents may come from teaching and research institutions in France or abroad, or from public or private research centers.

L'archive ouverte pluridisciplinaire **HAL**, est destinée au dépôt et à la diffusion de documents scientifiques de niveau recherche, publiés ou non, émanant des établissements d'enseignement et de recherche français ou étrangers, des laboratoires publics ou privés.

# Bulk modulus evolution of thermoset resins during crosslinking: Is a direct and accurate measurement possible?

Mael Péron, Vincent Sobotka, Nicolas Boyard  
and Steven Le Corre

## Abstract

The determination of the mechanical properties of thermoset resin and their evolution during transformation still represents a scientific issue in the composite materials community. A homemade apparatus named PvT $\alpha$  has recently been adapted to the measurement of neat resin bulk modulus evolution during cure and has been presented in a previous study. Several assumptions were used to directly obtain this value but they cannot be checked in situ. A multi-physic modelling of the system is proposed for this purpose in this paper. It accounts for the thermal, chemical and mechanical behaviours of the different components of the apparatus as well as their interactions during an experiment. This model is thoroughly validated thanks to several comparisons with experimental results. This study shows that the early assumptions are not verified during the whole cure in the case of RTM6 resin. It leads to 40% error in the bulk modulus estimation, thus making impossible a direct measurement of the resin bulk modulus using the simple protocol proposed by Nawab et al. A new procedure, which is based on the developed model, is proposed to improve the analysis accuracy.

## Keywords

Thermoset resin, mechanical properties, bulk modulus, curing, modelling, characterisation

## Introduction

Composite materials have known a growing use during the last decades in several industries such as aeronautics and automotive due to their lightness and interesting mechanical properties compared to aluminium and other metal-based alloys. However, their heterogeneous microstructure gives rise to residual stresses during cure, which is one of the major technological problems. These stresses may induce part defects during the manufacturing, such as shape distortions or matrix cracking.<sup>1–5</sup> A precise modelling of these stresses development would allow one to control and optimise the forming process, leading to time and cost savings and high quality parts. Several properties of the matrix and the fibres are required to feed these models, among which the matrix mechanical properties as well as the coefficient of thermal expansion (CTE), the coefficient of chemical shrinkage (CCS) and their relationship with the degree of cure appear to have a strong effect on the residual stresses development.<sup>3,6–8</sup> Numerous studies investigated CTE and CCS determination using several

instruments, which were reviewed by Nawab et al.<sup>9</sup> Resin mechanical properties are tricky to evaluate because the resin state changes during the transformation. Their characterisation still represents a scientific and technological challenge and remains the subject of multiple studies.<sup>10,11</sup> The bulk modulus  $K$  is of particular interest. It characterises the volumetric variation of a sample undergoing hydrostatic compressive pressure  $P$  under a fixed temperature  $T$  and degree of cure  $x$  and is defined by equation (1), where  $V$  is the volume.

$$K = -V \left. \frac{\partial P}{\partial V} \right|_{T,x} \quad (1)$$

Laboratoire de Thermocinétique de Nantes – UMR CNRS 6607, Polytech'Nantes, Nantes, France

### Corresponding author:

Mael Péron, Laboratoire de Thermocinétique de Nantes – UMR CNRS 6607, Polytech'Nantes, Bâtiment ISITEM, Rue Christian Pauc, 44306 Nantes, France.  
Email: [mael.peron@univ-nantes.fr](mailto:mael.peron@univ-nantes.fr)

When modelling the thermosetting resin mechanical behaviour, the bulk modulus links the stress tensor to the thermal expansion and chemical shrinkage strain tensors. As a consequence, it is of equal importance compared to the coefficients of thermal expansion and of chemical shrinkage when modelling the development of residual stresses in thermosetting resin during cure. Few studies attempted to evaluate the evolution of this modulus during cure. The first one is reported by Lindrose<sup>12</sup> who used ultrasonic waves propagation to measure the epoxy resin bulk and shear moduli evolution during its crosslinking. He reported an increase of the bulk modulus from 2.46 to 4.53 GPa in its liquid and solid states, respectively. He also assumed the existence of a linear relation between the bulk modulus evolution and the degree of cure. But as wave velocity is highly sensitive to temperature changes, the measurements were limited to quasi-isothermal and non-exothermic conditions. Due to the low temperature level, the tests took more than 24 h. Freemantle and Challis<sup>13</sup> also investigated the propagation of ultrasonic waves to measure the bulk modulus evolution of thermosetting adhesive specimens during cure. They measured a rise in the bulk modulus with a cured value comprised between 4.1 and 4.7 GPa depending on the initial formulation. Their study suffers from the same drawbacks as described for the previous investigation.<sup>12</sup> Dixon et al.<sup>14</sup> employed electromagnetic acoustic transducers to measure the shear and bulk moduli evolution with curing time. For their two epoxy resin formulations, the estimated bulk modulus evolved from 3.0 to 4.55 GPa and from 3.35 to 5.30 GPa, respectively, between the liquid and the solid state. The experimental conditions had to be the same as previously described<sup>12</sup> for the same reasons. Meng et al.<sup>15</sup> employed a pressurisable dilatometer to accurately evaluate the bulk modulus of liquid or glassy polymer samples evolution with temperature and pressure. Also, their experiments were only performed on thermoplastics. For these different methods,<sup>12–15</sup> no information on the degree of cure evolution was provided. Finally, Nawab et al.<sup>16</sup> proposed the use of a home-built apparatus, named PvT $\alpha$ , to simultaneously characterise several properties including the bulk modulus evolution of a vinylester resin sample with respect to the degree of cure. They reported a non-linear relation between the degree of cure and the bulk modulus. Its value increased from 0.25 GPa in the liquid state to 2.72 GPa in its solid fully cured state.

The method used by Nawab et al.<sup>16</sup> allows for the direct measurement of bulk modulus, CTE and CCS from experiments but relies on several assumptions. Even if results are in rather good agreement with literature, they may suffer from one over-simplifying assumption: the pressure applied on the sample is

considered as hydrostatic, allowing some shortcuts in the resin bulk modulus evaluation. As it is not possible to check such hypothesis in situ, further investigations are needed. The present study aims to verify numerically the stress state around the sample. Once it is known, it is possible to determine under which conditions the measured mechanical modulus is the actual or an apparent one. Finally, the question of the possibility to measure the actual modulus and at what cost is addressed. After a quick reminder of the PvT $\alpha$  characterisation method, the multi-physical model is stated and its solving and validation are detailed. Simulation results are then exposed, leading to discussions on the actual measurement system and its ability to capture bulk modulus evolution with cure.

## PvT $\alpha$ mould

### Description

The PvT $\alpha$  mould<sup>16–18</sup> is devoted to the study of neat thermosetting resins and their associated composite materials during and/or after curing cycle. Several physical quantities are simultaneously determined, including temperature, volume change and conversion degree for an applied pressure. Generally, the experiments are performed on bulk cylindrical samples with dimensions of 42 mm diameter and up to several millimetres thick. One of the main interests of this device is to apply conditions close to industrial ones, i.e. adjustable pressure up to 10 MPa and temperature up to 200°C. The mould consists of a piston, which can move in a cylindrical stainless steel cavity (Figure 1(a)) with a 50-mm internal diameter. It has been designed to ensure a unidirectional heat transfer through the sample thickness. The thermal control of the mould is performed by heaters located at the top and the bottom of the mould to heat the piston and the cavity, respectively. The cooling of the device is made by a circulation of compressed air in both parts of the mould. The mould is placed between the platens of an electric press so the position of the piston is adjusted in real time to apply the required pressure level. Two non-invasive heat flux sensors are placed in the bottom of the moulding cavity and in the piston. Data treatment provides temperature and heat flux density at the surface of the piston or the bottom of the cavity, exchanged between the sample and the mould. The resin sample is sealed in a low shear modulus elastomeric capsule (see Figure 1(b)) to avoid the leakage of the resin and the jamming of the mould. Resin injection inside the capsule is done with syringes and vacuum assistance to avoid air bubbles. The capsule is then placed in the moulding cavity. During an experimental run, a temperature cycle is imposed and the piston

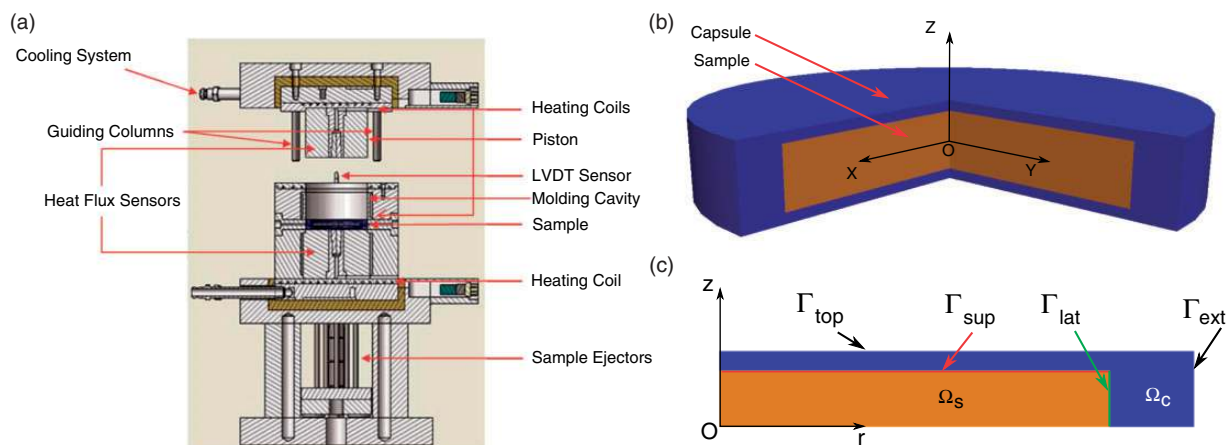


**Figure 1.** a) PvT $\alpha$  mould cross-section. b) Sectional view of the capsule and the sample. c) Geometrical simplification.

moves following the variations of the sample volume to get the desired pressure. Piston movements are recorded by a LVDT-type displacement sensor with a precision of 1  $\mu\text{m}$  and a range of 10 mm.

### Usual treatment and assumptions

One of the main considerations is that the elastomeric capsule containing the sample is considered as deformable but incompressible, so the pressure around the sample is assumed to be hydrostatic. It is simply treated like a perfect fluid. The measured thickness evolution is thus considered to be directly linked to the sample volume evolution. In order to remove the effect of thermal expansions of the mould and the silicone capsule from the overall measurement, a second experiment – called ‘baseline’ – is performed with a full cylindrical silicone sample, whose volume is equivalent to the volume of the used capsule. The baseline volume evolution is subtracted from the initial experiment volume evolution. This subtraction leads to the estimated volume variations of the sample only.<sup>16–18</sup>

In their conventional configuration, experiments are carried out under constant pressure to measure thermal expansion and chemical shrinkage coefficients together with the degree of cure. In their study, Nawab et al.<sup>16</sup> proposed to apply a specific cyclic pressure condition on a neat resin sample to determine some resin mechanical properties evolution during cure. Assuming that the stress around the sample remains hydrostatic during the experiment and knowing the sample volume variation, it is possible to directly estimate the sample bulk modulus evolution during crosslinking.

However, several assumptions could invalidate the proposed protocol if not verified. First of all, the capsule is considered as deformable enough to perfectly follow the sample dimensions. As a consequence, no voids are considered between the sample and the

capsule and both of them are stuck during the whole cure (Assumption 1). Then, the pressure around the sample is considered as hydrostatic, allowing one to determine directly the bulk modulus  $K$  from the volume variation under a pressure increment (Assumption 2). Finally, as the sample volume is estimated by subtracting the volume of an equivalent capsule from the volume of the capsule and the sample, one considers that the estimated sample volume and its variation under pressure are the same as the real sample ones (Assumption 3). As it is not possible to check experimentally, these assumptions in the available device, a numerical investigation is performed in the present work.

### Numerical modelling

To model the previous problem, it is essential to capture the thermal, chemical and mechanical states of the sample, the thermal and mechanical states of the capsule and the mechanical interactions between the mould, the capsule and the sample during the curing cycle. Nawab already showed that temperature gradients cannot be neglected in the apparatus study<sup>19</sup> due to possible high and rapidly released energy during cure. Thus, the volumes of the sample and the capsule have to be considered. Due to geometrical and boundary conditions symmetries, the problem can be simplified thanks to a vertical symmetry axis ( $Oz$ ) and a horizontal symmetry plane ( $xOy$ ), see Figure 1(b). Only one top half of the sample and the capsule are studied (see Figure 1(c)).

Due to the relatively small displacements observed during an experimental test, we consider that the sample and the capsule undergo small strain deformations. As a consequence, no heat generation due to plastic dissipation is considered. Self and frictional heating are also neglected compared to other heat sources, i.e. reaction exothermy, because the experiments are performed under quasi-static mechanical loadings. Thus,

thermal and mechanical problems can be uncoupled and only the thermal state will impact the mechanical one.

The multi-physical modelling is done using two main submodels: one dedicated to the thermo-chemical coupling and one to the mechanical behaviour. Both submodels are presented in the following paragraphs. First, the modelling of the thermo-chemical state of the sample and the capsule is presented, so as to determine temperature and reaction rate fields. Then, the modelling of mechanical interactions between the mould, the capsule and the sample is detailed. Knowing the previous thermal and chemical fields, the stress states and volume estimations are calculated. Finally, the solving of both physics is realised using the finite element method (FEM) to simulate the complete behaviour of the capsule and the sample during cure. The whole FEM formulation was developed and solved using FreeFem++.<sup>20</sup>

### Thermal and chemical modelling

The general heat conduction model (equation set 2) describes the heat transfer inside the capsule and the sample. The sample and capsule properties are denoted using the subscript 's' and 'c', respectively.

$$\begin{cases} \rho_s C p_s \frac{\partial T_s}{\partial t} = \nabla \cdot (\lambda_s \nabla T_s) + \rho_s \Delta H_s \frac{\partial x_s}{\partial t}, & \text{in } \Omega_s \\ \frac{\partial x_s}{\partial t} = F(T_s, x_s), & \text{in } \Omega_s \end{cases} \quad (2a)$$

$$\begin{cases} \rho_c C p_c \frac{\partial T_c}{\partial t} = \nabla \cdot (\lambda_c \nabla T_c), & \text{in } \Omega_c \end{cases} \quad (2b)$$

where  $\rho$  is the density,  $Cp$  is the specific heat,  $T$  is the temperature,  $x$  is the degree of cure,  $\lambda$  is the thermal conductivity and  $\Delta H_s$  is the reaction enthalpy.

A reaction heat source linked with the reaction rate is coupled to the heat conduction equation inside the sample equation (2a)<sub>1</sub>.<sup>21</sup> Reaction kinetics is governed by equation (2a)<sub>2</sub>, which depends on temperature and degree of cure.

A Fourier boundary condition is considered between the mould and the capsule (equation (3)<sub>1</sub>) and between the sample and the capsule (equation (3)<sub>3</sub>) to introduce a thermal contact resistance (TCR).

$$\begin{cases} -\lambda_c \nabla T_c \cdot \mathbf{n}_c = \frac{T_c - T_{ext}}{\gamma_{sup}}, & \text{on } \Gamma_{top} \\ -\lambda_c \nabla T_c \cdot \mathbf{n}_c = 0, & \text{on } \Gamma_{ext} \\ -\lambda_s \nabla T_s \cdot \mathbf{n}_s = \frac{T_c - T_s}{\gamma_{int}}, & \text{on } \Gamma_{sup} \cup \Gamma_{lat} \\ T_i(r, z, t = 0) = T_{ini}, & \text{with } i = c \text{ or } s \end{cases} \quad (3)$$

where  $\mathbf{n}_i$  is the normal vector on the outer surface,  $\gamma_{sup}$  is the TCR between the capsule and the mould,  $T_{ext}$  is the applied temperature cycle,  $T_{ini}$  is the initial

temperature and  $\gamma_{int}$  is the TCR value between the capsule and the sample. Symmetry conditions are imposed on the (Oz) and the (Or) axes, and an adiabatic condition is considered on  $\Gamma_{ext}$  (equation (3)<sub>2</sub>).

All the thermal properties of the sample depend on the degree of cure  $x_s$  and may depend on the temperature  $T_s$ . The thermal properties of the capsule also depend on the temperature  $T_c$ . The coupled problem to be solved is thus non-linear.

### Mechanical modelling

Numerous mechanical models exist to describe the mechanical behaviour of rubbers.<sup>22</sup> In this paper, a small strain linear elasticity model (equation set 4) is used. The elastomer capsule has a low shear modulus and has always been considered as incompressible. In fact its bulk modulus is lower than the one of the uncured resin. Thus, the sample and the elastomeric capsule are both considered as nearly-incompressible. A mixed formulation<sup>23</sup> was adopted to take this characteristic into account. Finally, these formulations take into account thermal expansion and a chemical shrinkage term is added to the sample mechanical formulation.

$$\begin{cases} \nabla \cdot \boldsymbol{\sigma}_c = 0, & \text{in } \Omega_c \\ \boldsymbol{\sigma}_c = 2\mu_c \boldsymbol{\varepsilon}_c^d - p_c \mathbf{I}, & \text{in } \Omega_c \\ \frac{-p_c}{K_c} = \text{tr}(\boldsymbol{\varepsilon}_c) + \text{tr}(\boldsymbol{\varepsilon}_c^{th}), & \text{in } \Omega_c \end{cases} \quad (4)$$

The sample is composed of neat thermosetting resin. In its initial state, the resin behaves as a deformable liquid unable of sustaining shear stress. When the cross-linking of the resin occurs, the shear modulus drastically rises<sup>6,12,14,24</sup> and the bulk modulus remains in the same order of magnitude but also increases.<sup>12-14</sup> Several phenomenological models have been developed to take into account development of the mechanical properties of thermosetting resins during cure.<sup>25-29</sup> In the present study, the mechanical behaviour retained is based on the small strain model developed by Hossain et al.<sup>28</sup> and is given by equation (5)<sub>2</sub>.

$$\begin{cases} \nabla \cdot \boldsymbol{\sigma}_s = 0, & \text{in } \Omega_s \\ \boldsymbol{\sigma}_s = \int_0^t 2\mu_s(\tau) \dot{\boldsymbol{\varepsilon}}_s^d(\tau) d\tau - \int_0^t \dot{p}_s(\tau) \mathbf{I} d\tau, & \text{in } \Omega_s \\ \frac{-p_s}{K_s} = \text{tr}(\boldsymbol{\varepsilon}_s) + \text{tr}(\boldsymbol{\varepsilon}_s^{th}) + \text{tr}(\boldsymbol{\varepsilon}_s^{ch}), & \text{in } \Omega_s \end{cases} \quad (5)$$

with

$$\boldsymbol{\varepsilon} = \frac{1}{2} (\nabla \mathbf{u} + \nabla^T \mathbf{u}), \quad \boldsymbol{\varepsilon}^d = \boldsymbol{\varepsilon} - \frac{1}{3} \text{tr}(\boldsymbol{\varepsilon}) \mathbf{I} \quad (6)$$

$$\boldsymbol{\varepsilon}^{th} = \alpha \Delta T \mathbf{I}, \quad \boldsymbol{\varepsilon}^{ch} = -\beta \Delta x \mathbf{I} \quad (7)$$

$$\dot{\boldsymbol{\varepsilon}} = \frac{\partial \boldsymbol{\varepsilon}}{\partial t} \quad (8)$$

where  $\boldsymbol{\sigma}$  represents the Cauchy stress tensor,  $\mu$  the shear modulus,  $\boldsymbol{\varepsilon}$  the strain tensor,  $\mathbf{u}$  the axisymmetric displacement field,  $p$  the pressure field,  $\mathbf{I}$  the identity matrix,  $K$  the bulk modulus,  $\boldsymbol{\varepsilon}^{th}$  the thermal strain tensor,  $\boldsymbol{\varepsilon}^{ch}$  the chemical strain tensor,  $\boldsymbol{\varepsilon}^d$  the deviatoric part of the strain tensor,  $\alpha$  the linear CTE,  $\beta$  the linear CCS,  $\Delta T$  the temperature difference with respect to the initial temperature,  $\Delta x$  the degree of cure increment and  $t$  the current time.

During the experiment, the load on the steel piston is controlled in order to follow the displacement of the upper surface of the capsule. It is considered as a rigid body, and its effect is accounted for by imposing a uniform displacement  $u_{piston}$  along the vertical on the top of the capsule (see Figure 1(c))

$$\begin{pmatrix} u_{rc} & u_{zc} \end{pmatrix} = \begin{pmatrix} 0 & u_{piston} \end{pmatrix} \quad (9)$$

On this boundary, displacements along the horizontal direction are fixed to zero, corresponding to a pure adhesion between the piston and the capsule (equation (9)). The imposed displacement  $u_{piston}$  is determined such as the equivalent force on the top of the capsule equals the desired imposed force  $F_{imp}$ , respecting the condition described by equation (10)

$$\int_{\Gamma_{sup}} (\boldsymbol{\sigma}_c \cdot \mathbf{n}_c) \cdot \mathbf{n}_c d\Gamma = F_{imp}(t) \quad (10)$$

A sliding contact along the vertical direction on the side of the capsule  $\Gamma_{ext}$  is considered. Due to the axisymmetry, displacements along the radial direction are blocked on the symmetry axis, and in the same way, displacements along the vertical direction are blocked on the horizontal symmetry plane. A perfect contact condition between the sample and the capsule is imposed on their interface. For a better modelling of this condition, a contact formulation should be adopted. We assume here a bilateral sticking contact so that the results of simulations presented thereafter hold only for compressive states at the interface and on the boundaries of the capsule. Fortunately, this will be the case for most of the PvT $\alpha$  loading conditions.

## Materials

### Elastomeric rubber

The capsule is composed of low shear modulus silicone rubber. The elastomeric rubber material was characterised using several techniques. First, its thermal properties and density evolution were determined using differential

**Table 1.** Elastomer properties.

Property	Value
$C_p$ (J.kg <sup>-1</sup> .K <sup>-1</sup> )	1.150.10 <sup>3</sup>
$\lambda$ (W.m <sup>-1</sup> .K <sup>-1</sup> )	0.25
$K$ (GPa)	0.58
$\mu$ (MPa)	1.0
$\alpha$ (10 <sup>-6</sup> K <sup>-1</sup> )	288.0

scanning calorimeter, guarded hot plate method and PvT $\alpha$  mould, respectively. This latter was also used to determine the rubber volume CTE, which value was validated compared to dilatometer results. Elastomer mechanical properties were measured at room temperature following ASTM D-575<sup>30</sup> and ASTM D-412<sup>31</sup> for bulk modulus and tensile modulus characterisation, respectively. Its shear modulus was obtained from the two previous moduli using the classical elasticity relations. The different properties are given in Table 1.

### RTM6 epoxy resin

The selected thermosetting resin is the HexFlow RTM6 epoxy resin from Hexcel composites. RTM6 is mainly dedicated to composite manufacturing for aeronautics and space industry. Thermal properties, density and reaction kinetic model (equation set 11) were determined by Lecoite.<sup>32</sup> In his work, Lecoite did not observe any effect of the temperature on the thermal conductivity. As a consequence, only the linear evolution of this property with the degree of cure is considered, based on his experimental results. PvT $\alpha$  mould in its classical experimental protocol was used to measure the volumetric liquid and cured resin CTEs and the volumetric CCS. These last data are consistent with results given by Aduriz et al.<sup>18</sup> In their work, they also investigated the evolution of the glass transition temperature  $T_g$  with degree of cure, which value in the uncured and fully cured states equals 258 and 493 K, respectively. Based on their model for the evolution of  $T_g$  with degree of cure and the results from the simulation presented in the section ‘Numerical results’, it appeared the temperature in the sample would exceed  $T_g$  only at the end of the chemical reaction, when the mean degree of cure reaches 0.95. Because this study mainly focuses on the resin behaviour during transformation, the effect of  $T_g$  has been disregarded in this study.

$$\begin{cases} \frac{dx}{dt} = F(T)G(x), & \text{in } \Omega_s \\ F(T) = F_{ref} e^{-A \left( \frac{T_{ref}}{T} - 1 \right)}, & \text{in } \Omega_s \\ G(x) = \sum_{i=0}^6 a_i \cdot x^i, & \text{in } \Omega_s \end{cases} \quad (11)$$

**Table 2.** RTM6 cure kinetics properties.<sup>32</sup>

Property	Value	Property	Value
$T_{ref}$ (K)	413	$a_2$	-20.712
$F_{ref}$	$2.569.10^{-4}$	$a_3$	66.2303
A	15.325	$a_4$	-116.075
$a_0$	0.02438	$a_5$	98.5327
$a_1$	5.07537	$a_6$	-33.0794

**Table 3.** RTM6 resin thermal properties.<sup>32</sup>

Property	RTM6 resin value
$C_p$ (J.kg <sup>-1</sup> .K <sup>-1</sup> )	$(1-x).C_{p_{liq}} + x.C_{p_{sol}}$
$C_{p_{liq}}$ (J.kg <sup>-1</sup> .K <sup>-1</sup> )	$C_{p_{liq}}(T(^{\circ}C)) = 1208.15 + 15.19T - 0.0497T^2$
$C_{p_{sol}}$ (J.kg <sup>-1</sup> .K <sup>-1</sup> )	$C_{p_{sol}}(T(^{\circ}C)) = 816.29 + 13.35T - 0.0377T^2$
$\lambda$ (W.m <sup>-1</sup> .K <sup>-1</sup> )	$(1-x).\lambda_{liq} + x.\lambda_{sol}$
$\lambda_{liq}$ (W.m <sup>-1</sup> .K <sup>-1</sup> )	0.10
$\lambda_{sol}$ (W.m <sup>-1</sup> .K <sup>-1</sup> )	0.22
$\Delta H$ (J.kg <sup>-1</sup> )	$410.10^3$

Tables 2 and 3 provide the parameters of the kinetic model and the thermo-physical properties of the resin, respectively.

Mechanical properties in the liquid and solid rubbery states have been studied in many experimental and numerical works.<sup>3,6-14,16,24-29</sup> Resin bulk modulus is generally considered as a linear function of the degree of cure

$$K(x) = (1-x).K_{liq} + x.K_{sol} \quad (12)$$

where subscripts *liq* and *sol* stand for the liquid and solid states, respectively.

The shear modulus develops after the gel point and sharply increases, as can be seen in several studies.<sup>6,12,14,24</sup> Before gelation, an arbitrary small value of the shear modulus is fixed at 5.0 Pa in order to facilitate the simulation. It was shown to have no effect on the results up to the gel point. Once it is reached, the shear modulus increases according to the following law

$$\left\{ \begin{array}{l} \mu(x) = \mu_{liq}, \\ \left\{ \begin{array}{l} \mu(x) = \mu_{liq} + 0.5.(\mu_{sol} - \mu_{liq}). \\ (1 + \tanh(\eta.(x - x_{tr}))) \end{array} \right\}, \end{array} \right. \quad \begin{array}{l} \text{when } x < x_{gel} \\ \text{when } x \geq x_{gel}. \end{array} \quad (13)$$

As the crosslinking occurs, the CTE of the resin is assumed to evolve linearly with the degree of cure

**Table 4.** RTM6 mechanical properties.

Property	Value	Property	Value
$K_{liq}$ (GPa)	2.5	$\mu_{liq}$ (MPa)	$5.0.10^{-6}$
$K_{sol}$ (GPa)	5.0	$\mu_{sol}$ (MPa)	5.0
$\alpha_{liq}$ ( $10^{-6}$ K <sup>-1</sup> )	190.0	$x_{gel}$	0.5
$\alpha_{sol}$ ( $10^{-6}$ K <sup>-1</sup> )	56.7	$\eta$	20.0
$\beta$ (%)	2.9	$x_{tr}$	0.8

following a mixture rule between its liquid and solid values

$$\alpha(x) = (1-x)\alpha_{liq} + x\alpha_{sol} \quad (14)$$

All the mechanical properties used in the resin models are gathered in Table 4. As no precise value was available in the literature, average values were chosen from the different studies concerning the development of mechanical properties of epoxy resins during cure.<sup>3,6-14,16,24-29</sup> Also, the different mechanical properties generally depend on the temperature, which is due to a modification of the molecular agitation as the temperature changes. As will be shown later, the chemical reaction happens during an isothermal step. This study focuses on the resin behaviour during transformation. As a consequence, the temperature dependence of the mechanical properties is neglected in this work.

For both materials, the density is given by equation (15)

$$\rho = \frac{\rho_0}{(1 + tr(\epsilon))} \quad (15)$$

where  $\rho_0$  corresponds to the initial density at room temperature for the rubber capsule ( $\rho_0 = 1.112 \cdot 10^3$  kg.m<sup>-3</sup>) and to the liquid state density at room temperature for the RTM6 resin ( $\rho_0 = 1.117 \cdot 10^3$  kg.m<sup>-3</sup>). As the trace of the strain tensor  $tr(\epsilon)$  depends on thermal expansion and chemical shrinkage of the resin for the sample and on thermal expansion of the rubber for the capsule, the density depends on both the temperature and the degree of cure.

## Model validation

One experiment was performed with the PvT $\alpha$  mould in standard configuration (i.e. constant applied pressure) in order to validate the numerical model. The sample was composed of an 8.718 g ( $\pm 0.5$  mg) RTM6 resin sample encapsulated in an 8.570 g ( $\pm 0.5$  mg) elastomeric capsule.

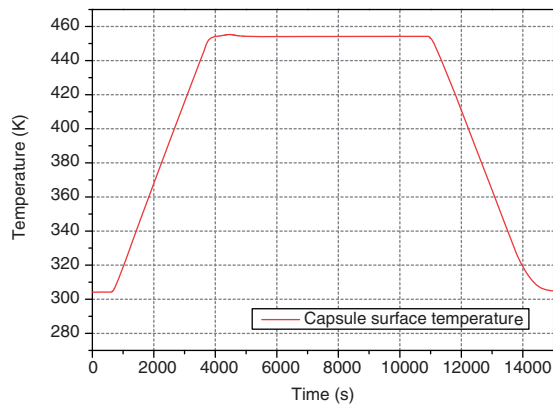


**Figure 2.** Imposed temperature cycle.

### Experimental protocol

The experiment was performed under a constant pressure of 2.0 MPa. The evolution of the capsule surface temperature with time is represented in Figure 2.

This temperature was determined by analysing the heat flux sensors data during the experiment.<sup>16–18</sup> It was then used as a boundary condition for the numerical modelling.

### Spatial and time discretisation convergence

FEM imposes to spatially and temporally discretise the phenomena to be simulated. Both discretisations may have an impact on solutions: a too coarse one and singularities may appear or events may be ignored. A too fine one leads to relatively high computer cost. Spatial discretisation was checked using several meshes and led to an optimal mesh of 1069 nodes for the sample mesh and 820 nodes for the capsule mesh. The use of a quasi-incompressible approach implies to choose adequate finite elements in order to avoid locking of the elements. P1+/P1 interpolation<sup>33</sup> was chosen here for the displacement/pressure fields in both the sample and the capsule discretisations.

Time discretisation was performed using a backward Euler integration scheme. Using the previous meshes, it was checked with different time increments from 0.25 to 32.0 s. According to the convergence results, the use of a small time increment during cure reaction is crucial. Time step control is thus performed at each time step using criteria based on temperature and degree of cure variations. The algorithm leads to time step of the order of 1.0 s during critical phases, ensuring an accurate simulation. Outside these phases, time increment may be increased to 32 s without inducing significant errors.

### Validation of the sample volume evolution

The validation consists in comparing the evolution of the experimental sample volume to the numerical one.

Both are plotted in Figure 3 together with the numerical degree of cure in the sample core and the imposed surface temperature.

After the first isothermal step at 30°C, the volume evolves linearly with the temperature rise during the heating step. The crosslinking starts at the end of this step and induces the chemical shrinkage. Thus, the whole transformation occurs during the first 30 min after the beginning of the isothermal step. No volume variation is observed after the degree of cure reaches the maximal value. During the cooling step, the volume evolves once again linearly with respect to the temperature variation. Unexpectedly, the experimental volume increases at the end of the cooling, which is attributed to an artefact of the system. It will not be taken into account in the following study since it occurs after the reaction.

The modelled cure shrinkage seems to develop slightly quicker than the experimental one, meaning that the numerical cure reaction rate described in the model given by Lecoite<sup>32</sup> overestimates the experimental one. Nevertheless, the model clearly matches the sample volume evolution and shows that experimentally determined CTE and CCS values allow for a reliable simulation of experimental sample behaviour.

### Complementary validations

A complementary validation is done, comparing the numerical heat flux density and the experimental one<sup>16–18</sup> (Figure 4).

A good agreement can be observed between both heat flux density curves. Slight differences (i.e. lower than  $250 \text{ W}\cdot\text{m}^{-2}$ ) during the exothermal reaction may be attributed to the non-perfectly one-dimensional heat transfer in the  $PvT\alpha$  and to the fact that the kinetic model is not accurate enough as observed for shrinkage.

Finally, it was possible to compare the experimental and numerical final shapes of the sample. Using a KEYENCE LJ-V7080 contactless profilometer, the lateral side profile was scanned and compared to the numerical one as presented in Figure 5. Once again, there is a very good agreement between the predicted and the measured data. A localised perturbation can be observed in a zone where a little default in the capsule fabrication leads to a surface slot on the sample lateral side. Outside this zone, the error between the predicted and the measured profile is lower than 1%.

The model being now fully validated in the classical  $PvT\alpha$  configuration, it can be used to check the system ability to identify the bulk modulus evolution of the thermoset resin during cure under a cyclic pressure condition. The conclusions of Nawab et al.<sup>16</sup> will thus be revisited, as their results were based on hypothesis that are not experimentally checkable.

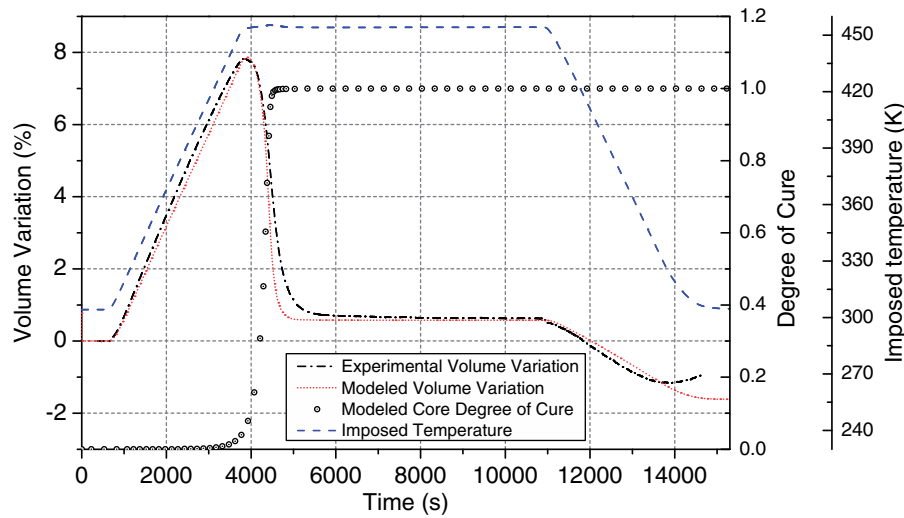


Figure 3. Comparison between experimental and modelled volume for the resin sample.

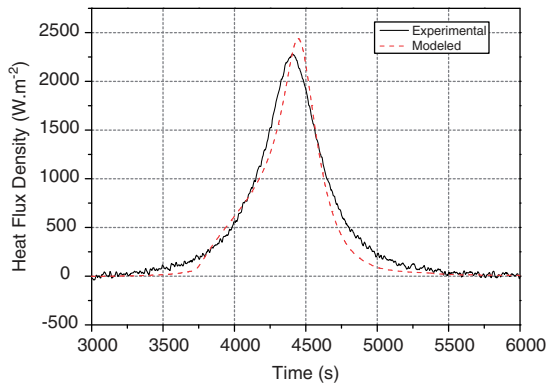


Figure 4. Comparison between the experimental and the modelled heat flux densities.

## Numerical results

### Stress state around the sample

By analysing the stress state around the sample, it is now possible to verify the two first assumptions posed by Nawab et al.<sup>16</sup> The criterion on which is based the following study is the ratio of the lateral surface mean normal stress over the superior surface mean normal stress around the sample

$$\chi = \frac{\sigma_{lat}}{\sigma_{sup}} \quad (16)$$

When the sample is under an isotropic state of stress, these two mean stresses are equal, leading to a mean stresses ratio  $\chi$  equal to one. If it tends to zero, it means that the lateral side of the sample tends to unstick from the capsule surface (Figure 6). Conversely, this ratio tends to an infinite value if the top or bottom surface

of the sample tends to lose the contact (Figure 6). A negative value means that one of the two surfaces undergoes tension when the other one is under compressive stress. The surface under tension would lead to an unsticking between the capsule and the sample, which would introduce an error in the sample volume evolution measurement. As mentioned above, this situation can easily be identified from simulations and disregarded in most cases.

If  $\chi$  differs from unity, the volume variation associated to a pressure increment would be linked to both volumetric and deviatoric strains. As a consequence, the volume variation of the sample would be governed by the resin bulk and shear moduli  $\mu_s$  and  $K_s$ , respectively. Several simulations were performed in order to observe these phenomena, which are not presented here. The relation used by Nawab et al.<sup>16</sup> to determine the bulk modulus from the volume variation of the sample would, therefore, not hold. Commonly, the value of the stress ratio comprises between 1 and 0.

This ratio evolution with time from the previous simulation results is plotted in Figure 7, together with the degree of cure in the sample core and the shear and bulk moduli evolutions.

As clearly observed from Figure 7,  $\chi$  equals one during the first part of the reaction when the resin sample is still in its liquid state. The bulk modulus evolution does not seem to affect this ratio during this first step. As soon as the shear modulus of the sample develops, the stress ratio decreases, leading to a non-hydrostatic state of stress. Two phenomena linked to the degree of cure evolution occur at the same time and lead to this loss of hydrostaticity. First, the mechanical properties of the sample develop, making it able to sustain shear stresses; second, the sample volume shrinks due to the crosslinking, which lowers the compressive

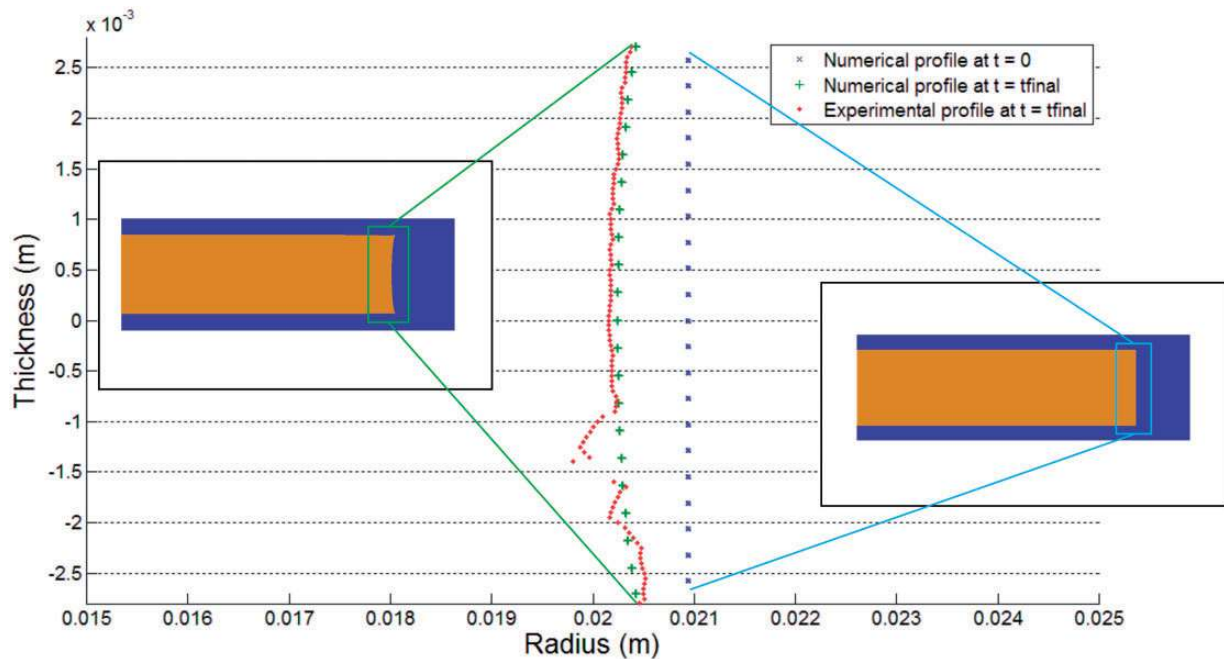


**Figure 5.** Comparison between the numerical and experimental sample profiles.

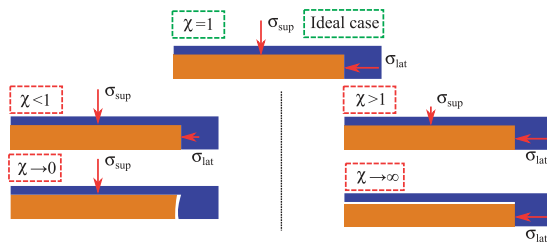


**Figure 6.** Capsule and sample surface contact situations for different values of the stress ratio  $\chi$ .

stress on the side of the sample. Due to the solid elastic nature of the capsule, the applied normal stress through the piston is not transferred homogeneously. Even for a constant pressure level of 2.0 MPa, the stress ratio decreases, implying a non-hydrostatic pressure condition.

The PvT $\alpha$  mould being commonly used under a constant pressure ranging between 0.2 and 6.0 MPa, one may have to check if unsticking can appear for these different pressure values. The time evolution of  $\chi$  under several pressure levels between 0.1 and 6.0 MPa is plotted in Figure 8(a) together with the degree of cure in the sample core.

For any pressure level,  $\chi$  is equal to one as the sample is in the liquid state and then decreases as soon as the degree of cure reaches the gel point. In order to limit the stress ratio decrease, it is necessary to apply a higher pressure on the capsule since  $\chi$  tends to 1 when the pressure increases (Figure 8(b)). On the

contrary, a lower pressure leads to a higher decrease of  $\chi$  and even a possible unsticking between the sample and the capsule for a pressure level lower than 0.17 MPa. This last phenomenon was already observed during experimental tests, where a too low pressure led to inconsistent results concerning the CTE and CCS measurements. As a first conclusion, a minimum pressure level is required in order to avoid sample unsticking and thus a misinterpretation of the CTE and CCS evaluation, verifying the assumption 1. Furthermore, the state of stress in the sample is also checked to be very sensitive to the cure degree, so that a too low pressure will combine the effects of  $K_s$  and  $\mu_s$ , promoting the deviatoric effects. In such conditions, the bulk modulus is not anymore correctly identified by the PvT $\alpha$  device.

### Bulk modulus determination

In order to determine the bulk modulus evolution of the sample during its cure and following the protocol described in Nawab et al.,<sup>16</sup> one has to apply a hydrostatic pressure cycle on the sample and to record its volume variation. The pressure cycle initially proposed by Nawab et al.<sup>16</sup> is described in Figure 9 and is repeated during the whole cure cycle every 80 s.

The pressure cycle proposed by Nawab et al. was ranging between 0.75 and 6.0 MPa. According to Figure 8, this range does not allow for a hydrostatic pressure condition around the sample, as the stresses ratio may fall to 0.82 when the pressure equals

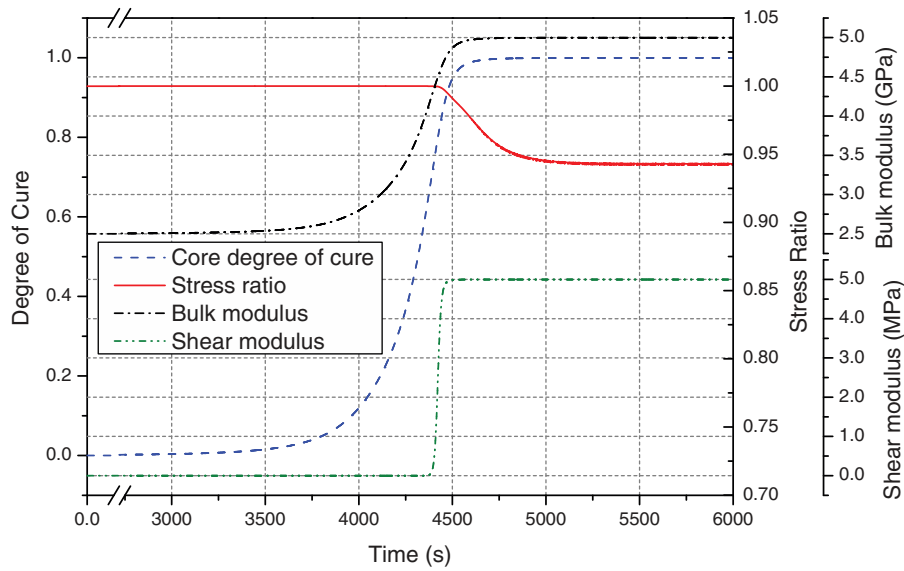


**Figure 7.** Stress ratio evolution with time for a 2.0 MPa pressure, with degree of cure at the sample core and bulk and shear moduli evolutions.

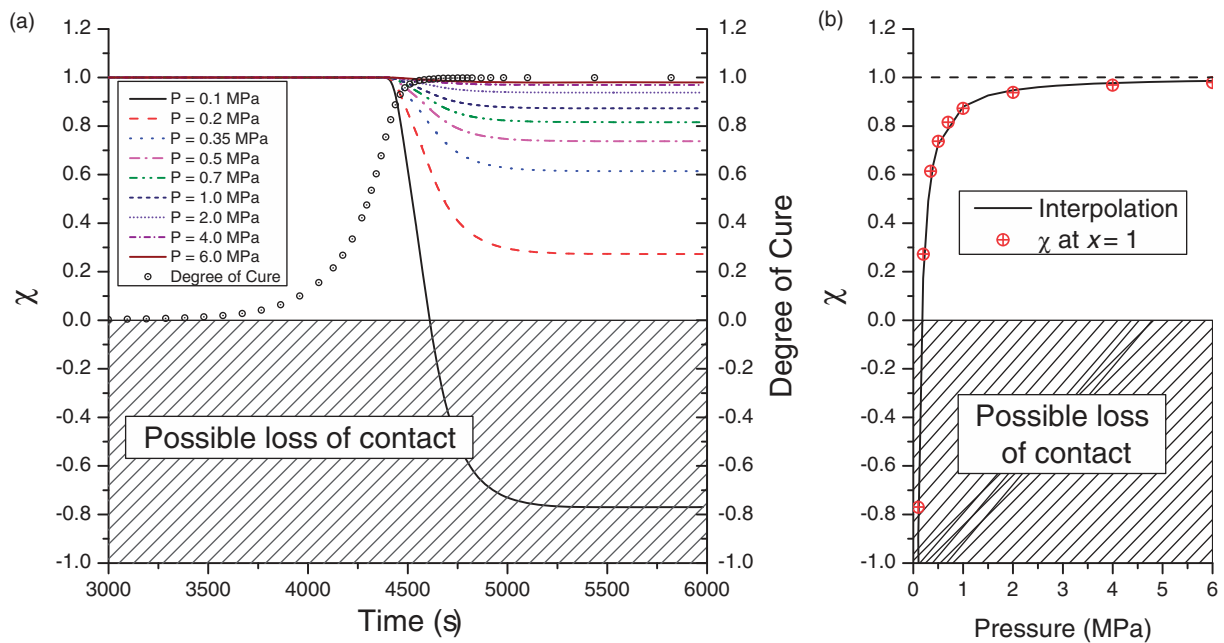


**Figure 8.** a) Time evolution of the stress ratio  $\chi$  for different pressure levels. b) Final stress ratio for different pressure levels.

0.75 MPa. To circumvent this defect and maintain a hydrostatic pressure around the sample, a new pressure cycle ranging between 5.0 and 10.0 MPa is proposed in Figure 9. This proposed pressure cycle verifies Assumption 2 during the whole transformation, when the pressure cycle used by Nawab et al. did not.

As already stated, the sample is encapsulated in a deformable capsule so that it is not possible to directly measure the sample volume  $V_S$  evolution during cure. In the protocol described by Nawab et al.,<sup>16</sup> a baseline

is performed on a bulk silicone sample, which volume is the same as the initial capsule one. The same temperature and pressure cycles are imposed. This volume baseline  $V_{BL}$  is subtracted from the resin sample and capsule volume variation  $V_{TOT}$  to extract an estimated sample volume evolution  $\tilde{V}_S$  only

$$\begin{cases} V_{TOT} = V_S + V_C \\ \tilde{V}_S = V_{TOT} - V_{BL}, \end{cases} \quad (17)$$

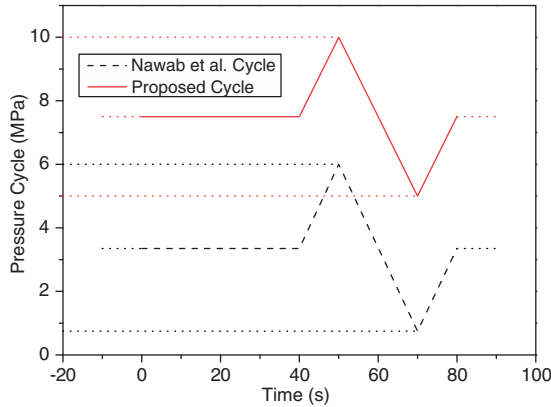


**Figure 9.** Nawab et al.<sup>16</sup> and the new proposed pressure cycles.

where  $V_C$  is the volume of the actual capsule. According to Assumption 3, the equality between  $V_C$  and  $V_{BL}$  would be verified and as a consequence of equation (17), the one between  $\tilde{V}_S$  and  $V_S$  would hold. The following paragraphs aim in studying this third assumption.

Using the developed multi-physics model, these two experiments (i.e. one on the sample and the capsule and another one on the equivalent capsule) proposed by Nawab et al. were numerically reproduced and used as an input in the bulk modulus estimation protocol, thus simulating numerically the experimental approach. The temperature cycle and properties are the same as used in the ‘Model validation’ section, and the pressure cycle is the new one previously proposed in Figure 9. The relative variation of the estimated sample volume, the imposed temperature cycle, the core and surface degrees of cure and the stresses ratio evolutions are plotted in Figure 10 for these simulations.

The global evolution of the sample volume is qualitatively the same as described in the ‘Sample Volume Evolution Validation’ section, except that one can observe periodical variations corresponding to the repeated pressure cycles. The stresses ratio  $\chi$  slightly decreases with the degree of cure from 1 to 0.98. The pressure is not perfectly hydrostatic around the sample but is thought acceptable. From these simulations and using the analysis method proposed by Nawab et al.,<sup>16</sup> it is thus possible to have an estimation of the time evolution of the bulk modulus and to compare it with the real one (i.e. numerically imposed) as plotted in Figure 11. The degree of cure is estimated from the heat flux density analysis.

As clear from this figure, the estimated values are in the same order of magnitude as the input one, but some differences appear between both moduli. When the resin is fully liquid and in the isothermal state (zone A), the estimated modulus is close to the real one, with an error lower than 0.7%. During heating

(zone B), the error increases and rises to 19%. The error reaches a maximum value of 43% during the cross-linking (zone C). After transformation and under isothermal conditions (zone D), the estimated modulus is higher than the real one, with an 8% error. Even though the sample is under a hydrostatic pressure condition, there is still an important error in the bulk modulus evaluation. This error is first attributed to the difference between the volume evolution of the actual capsule and the equivalent capsule under one pressure cycle. For each pressure increment  $\Delta P$  between the higher and the lower pressure level (in our case, between 10.0 and 5.0 MPa), and knowing the sample volume variation  $\Delta V_S$ , the bulk modulus  $K_S$  is calculated using the incremental formulation of equation (1)

$$K_S = -V_S \left. \frac{\Delta P}{\Delta V_S} \right|_{T,\alpha} \quad (18)$$

However,  $\Delta V_S$  is calculated from equation (17), leading to  $\Delta \tilde{V}_S$ . As illustrated in Figure 12, the difference between  $\Delta V_C$  and  $\Delta V_{BL}$  explains the observed discrepancies of Figure 11.

There are no differences during phase A or at the beginning of phase B. Curves then deviate during the heating, the real capsule volume variation being higher than the equivalent one. During the transformation (phase C), the high variations of the real capsule volume are due to the combination of temperature rise and chemical shrinkage. Finally, after the reaction and during the isothermal step (phase D), there is a constant difference between both volume variations. All these differences are due to the discrepancies between the real capsule and the equivalent capsule stress states. For the three times  $t_1$ ,  $t_2$  and  $t_3$  indicated on Figure 12 and corresponding to an applied pressure of 7.5 MPa, which is the average pressure of the cycle, the pressure distribution in the actual capsule is given in Figure 13.

At time  $t_1$ , the pressure distribution is uniform. The mechanical behaviours of the actual capsule and the bulk silicone sample used as baseline are the same. As the temperature rises, the deviatoric part of the state of stress increases leading to a heterogeneous pressure distribution inside the capsule (time  $t_2$ ). It then drastically changes during reaction, inducing a completely non-uniform pressure distribution with important pressure variations at time  $t_3$ , after the end of the reaction.

This heterogeneity is driven by the kinematics between the capsule and the sample. Several simulations were performed, which are not detailed here, leading to the following observations. During heating, the capsule drives the deformations inside the moulding cavity as its shear modulus is the highest one. The temperature rise, the capsule geometry and the difference between the sample and the capsule CTEs lead to the

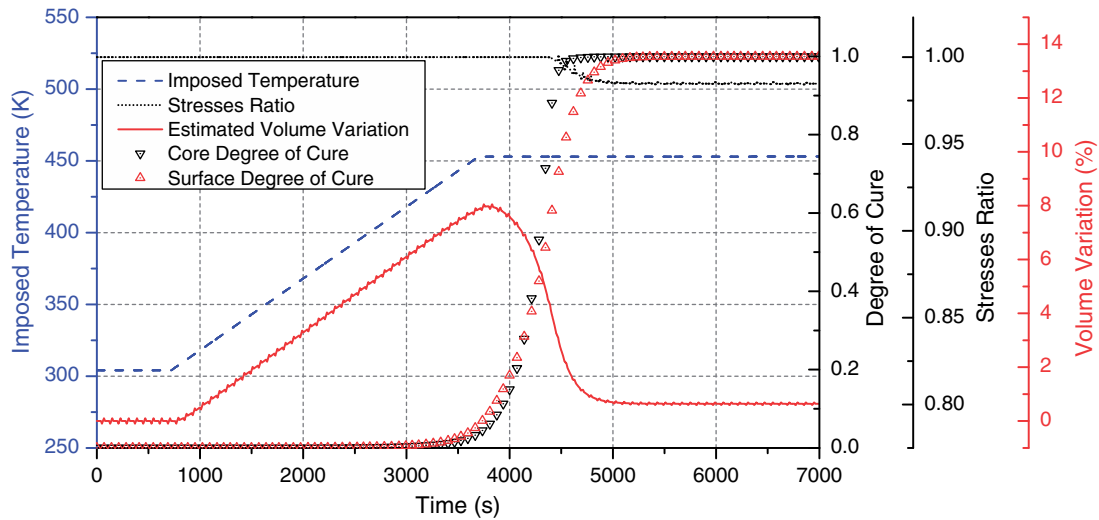


**Figure 10.** Estimated sample volume variation, imposed surface temperature, surface and core degree of cure and stresses ratio for the pressure cycle numerical experiment.

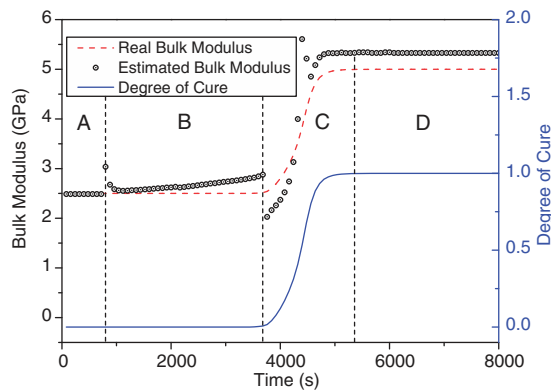


**Figure 11.** Comparison between the estimated and actual bulk moduli together with the degree of cure evolution.

nonuniform pressure distribution at time  $t_2$ . Finally, as reaction occurs, the sample shear modulus increases and overtakes the capsule shear modulus. The sample thus becomes the deformation driver and as shrinkage occurs it imposes its deformations to the capsule, leading to a heterogeneous pressure distribution. The estimated modulus outside the transformation (zones A, B and D) is nevertheless in good agreement with the actual one, the error being lower than 10% and due to a drift in the capsule mechanical behaviour.

During the transformation (zone C), which is the zone of main interest in this study, an additional error is also induced by thermal and chemical gradients. As the temperature used in Nawab et al.<sup>16</sup> protocol corresponds to the capsule surface temperature and the overall degree of cure is calculated from the heat flux sensors, no specific treatment is performed when high temperature and degree of cure gradients exist.

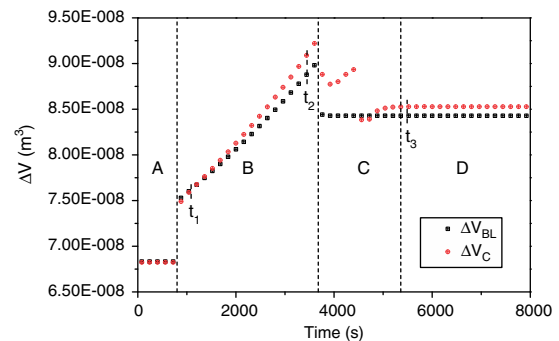


**Figure 12.** Comparison between the computed volume variation  $\Delta V$  under one pressure cycle of the actual capsule and the equivalent one.

In the case of the RTM6 resin, the cure cycle is a ramp to 180°C at 3 K.min<sup>-1</sup>, leading to a reaction which starts at 140°C. This leads to a high energy release in a short time due to a fast reaction. As a consequence, temperature and degree of cure differences reach 40°C and 0.27, respectively, between the core and the surface of the sample. To circumvent this phenomenon, it is possible to decrease the heating rate, which will lower the reaction rate. As the energy released is the same and the reaction rate is decreased, temperature and degree of cure gradients will be limited. Results for four different cure cycles with heating rates of 3, 2, 1 and 0.5 K.min<sup>-1</sup> are shown in Figure 14. The pressure cycle is the new one proposed in Figure 9 and the bulk modulus estimation method is the same as described for Figure 11.

The results confirm the fact that the protocol proposed by Nawab et al.<sup>16</sup> gives good estimations of the bulk modulus provided the thermal and chemical



**Figure 13.** Pressure distribution in the real capsule for different times. The sample is not represented for the sake of simplicity.

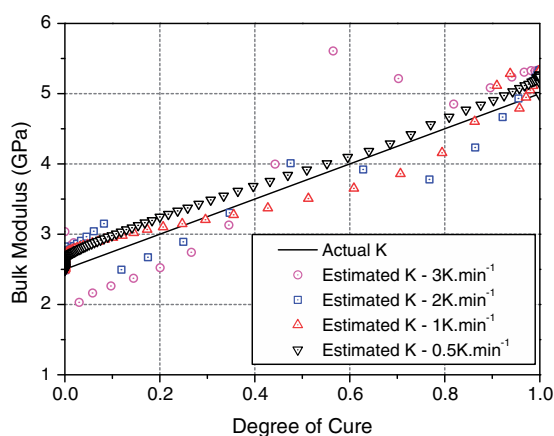


**Figure 14.** Bulk modulus evaluation for different heating rates as a function of degree of cure.

gradients are limited. When heating at  $0.5 \text{ K} \cdot \text{min}^{-1}$ , temperature and degree of cure differences between the surface and core of the sample are limited to  $10^\circ\text{C}$  and  $0.09$ , respectively. The estimation error during crosslinking is thus lower, its maximum value being  $8.2\%$ . The final error value equals  $5.2\%$ . The evolution with  $\alpha$  is found to be linear, with a quasi-constant gap of  $0.25 \text{ GPa}$  between the estimated and the actual  $K$ .

Reducing the heating rate might, however, not be an interesting solution as the heat flux during the transformation may not be high enough to be recorded by the heat flux sensors and may lead to an inaccurate degree of cure evolution. As a consequence, the estimation method have to deal with thermal and degree of

cure gradients if one wants to accurately determine the bulk modulus evolution during transformation.

## Conclusion

In previous studies dealing with the PvT $\alpha$  device, this apparatus was assumed to have the ability of providing mechanical information during curing of thermoset resin samples. A quite complex experimental procedure was proposed<sup>16</sup> to directly determine the bulk modulus  $K$  versus degree of cure  $\varphi$  and temperature  $T$ . However, the early assumptions used to estimate this value were impossible to be checked experimentally. This work thus presents a numerical approach that provides a better understanding and highlights some defects of the proposed experimental method. A multi-physics finite elements simulation tool was developed in order to verify them. It deals with difficult mechanical and thermal contact problems in confined situation, with quasi-incompressible materials, whose properties may strongly vary during transformation. The models were validated compared to several experimental results. Results show that the usual assumptions are not verified during the whole cure cycle in the case of RTM6 resin sample under a pressure in the range proposed by Nawab et al.<sup>16</sup> The bulk modulus estimation error outside the transformation is lower than  $8\%$  but can reach  $40\%$  during the crosslinking, due to thermal and chemical gradients and to the capsule mechanical behaviour. A decrease of the heating rate leads to a lower error during the transformation, with a maximal value of  $8.2\%$ , but may experimentally lead to an inaccurate estimation of the degree of cure. The developed

numerical model is a useful tool to predict the sample behaviour and to find the ideal thermal and pressure cycles in order to identify the bulk modulus. However, a new identification protocol is needed, which would take into account thermal and chemical gradients, as well as the complex mechanical behaviour of the capsule. Upcoming efforts will be put on the development of an inverse algorithm based on this model allowing for an accurate estimation of this property during cure, as already developed for the CTE and CCS identification.<sup>34</sup> An improvement of the model is also considered in order to take into account the effect of the glass transition temperature on the physical properties of the resin.

### Acknowledgements

The authors wish to associate the industrial partners of this project; respectively Airbus Group, Airbus Group Innovations, Daher and Solvay.

### Declaration of Conflicting Interests

The author(s) declared no potential conflicts of interest with respect to the research, authorship, and/or publication of this article.

### Funding

The author(s) disclosed receipt of the following financial support for the research, authorship, and/or publication of this article: this study is part of the COMPETH project supported by IRT Jules Verne (French Institute in Research and Technology in Advanced Manufacturing, Technologies for Composite, Metallic and Hybrid Structures).

### References

- Albert A and Fernlund G. Spring-in and warpage of angled composite laminates. *Compos Sci Technol* 2002; 62: 1895–1912.
- Svanberf JM and Holmberf JA. Prediction of shape distortions. Part II: experimental validation and analysis of boundary conditions. *Compos A Appl Sci Manuf* 2004; 35: 723–734.
- Wisnom MR, Gigliotti M, Ersoy N, et al. Mechanisms generating residual stresses and distortion during manufacture of polymer–matrix composite structures. *Compos A Appl Sci Manuf* 2006; 37: 522–529.
- Low IM. Effects of residual stresses on the failure micro-mechanisms in toughened epoxy systems. *J Mater Sci* 1990; 25: 2144–2148.
- Sirivedin S, Fenner DN, Nath RB, et al. Matrix crack propagation criteria for model short-carbon fibre/epoxy composites. *Compos Sci Technol* 2000; 60: 2835–2847.
- Bogetti TA and Gillespie JW. Process-induced stress and deformation in thick-section thermoset composite laminates. *J Compos Mat* 1992; 26: 626–660.
- White SR and Kim YK. Process-induced residual stress analysis of AS4/3501-6 composite material. *Mech Compos Mat Struct* 1998; 5: 153–186.
- Msallem YA, Jacquemin F, Boyard N, et al. Material characterization and residual stresses simulation during the manufacturing process of epoxy matrix composites. *Compos A Appl Sci Manuf* 2010; 41: 108–115.
- Nawab Y, Shahid S, Boyard N, et al. Chemical shrinkage characterization techniques for thermoset resins and associated composites. *J Mater Sci* 2013; 48: 5387–5409.
- Kravchenko OG, Li C, Strachan A, et al. Prediction of the chemical and thermal shrinkage in a thermoset polymer. *Compos A Appl Sci Manuf* 2014; 66: 35–43.
- Baran I, Akkerman R and Hattel JH. Material characterization of a polyester resin system for the pultrusion process. *Compos B Eng* 2014; 64: 194–201.
- Lindrose AM. Ultrasonic wave and moduli changes in a curing epoxy resin. *Exp Mech* 1978; 18: 227–232.
- Freemantle RJ and Challis RE. Combined compression and shear wave ultrasonic measurements on curing adhesive. *Meas Sci Technol* 1998; 9: 1291–1302.
- Dixon S, Jaques D and Palmer SB. The development of shear and compression elastic moduli in curing epoxy adhesives measured using non-contact ultrasonic transducers. *J Phys D Appl Phys* 2003; 36: 753–759.
- Meng Y, Bernazzani P, O'Connell PA, et al. A new pressurizable dilatometer for measuring the time-dependent bulk modulus and pressure-volume-temperature properties of polymeric materials. *Rev Sci Instrum* 2009; 80: 053903.
- Nawab Y, Casari P, Boyard N, et al. Characterization of the cure shrinkage, reaction kinetics, bulk modulus and thermal conductivity of thermoset resin from a single experiment. *J Mater Sci* 2013; 48: 2394–2403.
- Boyard N, Vayer M, Sinturel C, et al. Analysis and modeling of PVTX diagram of an unsaturated polyester resin, thermoplastic additive, and mineral fillers blend. *J Appl Polym Sci* 2003; 88: 1258–1267.
- Aduriz XA, Lupi C, Boyard N, et al. Quantitative control of RTM6 epoxy resin polymerisation by optical index determination. *Compos Sci Technol* 2007; 67: 3196–3201.
- Nawab Y, Tardif X, Boyard N, et al. Determination and modelling of the cure shrinkage of epoxy vinylester resin and associated composites by considering thermal gradients. *Compos Sci Technol* 2012; 73: 81–87.
- Hecht F. New development in Freefem++. *J Numer Math* 2012; 3–4: 251–266.
- Boyard N, Sobotka V and Delaunay D. Theoretical modeling of the curing process. In: Thomas S, Sinturel C and Thomas R (eds) *Micro- and nanostructured epoxy/rubber blends*. Weinheim: Wiley, 2014, pp.105–126.
- Holzappel GA. *Nonlinear solid mechanics*. Chichester: Wiley, 2000.
- Zienkiewicz OC. *The finite element method: its basis and fundamentals*, 6th ed. Oxford: Elsevier, 2005.
- O'Brien DJ, Mather PT and White SR. Viscoelastic properties of an epoxy resin during cure. *J Compos Mat* 2001; 35: 883–904.
- Adolf D and Martin JE. Calculation of stresses in cross-linking polymers. *J Compos Mat* 1996; 30: 13–34.

26. Van't Hof C. *Mechanical characterization and modeling of curing thermosets*. PhD Dissertation, TU Delft, Delft University of Technology, Delft, 2006.
27. Lion A and Höfer P. On the phenomenological representation of curing phenomena in continuum mechanics. *Arch Mech* 2007; 59: 59–89.
28. Hossain M, Possart G and Steinmann P. A small-strain model to simulate the curing of thermosets. *Comput Mech* 2009; 43: 769–779.
29. Hossain M and Steinmann P. Degree of cure-dependent modelling for polymer curing processes at small-strain. Part I: consistent reformulation. *Comput Mech* 2014; 53: 777–787.
30. ASTM D575-91:105-107. Standard Test Methods for Rubber Properties in Compression, ASTM International, West Conshohocken, PA, 2012, www.astm.org.
31. ASTM D472-68:92-102. ASTM D412-15a, Standard Test Methods for Vulcanized Rubber and Thermoplastic Elastomers–Tension, ASTM International, West Conshohocken, PA, 2015, www.astm.org.
32. Lecointe D. *Caractérisation et simulation des processus de transferts lors d'injection de résine pour le procédé RTM*. PhD dissertation, Université de Nantes, Nantes, 1999.
33. Arnold DN, Brezzi F and Fortin M. A stable finite element for the stokes equations. *Calcolo* 1984; 21: 337–344.
34. Tardif X, Agazzi A, Sobotka V, et al. A multifunctional device to determine specific volume, thermal conductivity and crystallization kinetics of semi-crystalline polymers. *Polym Testing* 2012; 31: 819–827.